

## SUBLIMATION OF NITRIC OXIDE FILMS: ROTATIONAL AND ANGULAR DISTRIBUTIONS OF DESORBING MOLECULES

D.F. PADOWITZ and S.J. SIBENER

*The James Franck Institute and The Department of Chemistry, The University of Chicago, Chicago, IL 60637, USA*

Received 29 December 1988; accepted for publication 27 February 1989

NO molecules subliming into vacuum from a condensed NO film at 50 K exhibit cosine angular flux and Boltzmann rotational distribution at the surface temperature. This implies that the sticking probability for incident molecules is independent of angle or rotational energy, at least for levels populated at 50 K. We look at some models for rotational distributions of desorbing molecules, and consider the extent to which desorption can be used as a probe of the surface dynamics of condensed phases. Though our results are simple, they touch on issues fundamental to obtaining microscopic dynamical information for non-equilibrium interfaces.

### 1. Introduction

A century ago, Hertz [1] used gas kinetic theory to predict a maximum rate for evaporation. Deviations from this rate caused Marcelin [2] and Knudsen [3] to propose a sticking coefficient, an idea suggested originally by Maxwell [4]. We have returned to the question of sticking in evaporation or sublimation, among the earliest problems in surface science, to see what we can learn from measurements of state resolved desorption distributions. We find that ultrahigh vacuum (UHV) techniques are applicable to subliming or evaporating materials when the vapor pressure is sufficiently low, and under such conditions we can expect quasi-equilibrium at the surface. We will briefly consider the breakdown of local equilibrium, and the importance of state resolved sticking dynamics at non-equilibrium interfaces. In contrast to the often complex results of desorption from low coverage adsorbates on crystal surfaces [5,6], we observe simple Boltzmann and cosine distributions. Rigorously, we can conclude only that the sticking probability for equilibrium gas molecules on a 50 K NO surface is independent of angle or rotational level. Nevertheless, we believe that the *absence* of dynamical effects may indicate a gas-like surface species or precursor to desorption.

## 2. Experimental

The UHV [7], and laser systems [8], have been described previously. The UHV chamber had a base pressure of  $< 1 \times 10^{-10}$  Torr. A single crystal metal substrate mounted on a sample manipulator was cooled by a liquid helium cold tip and resistively heated. The sample was dosed from one of two molecular beam sources. The angular distribution of desorbing species was measured with a mass spectrometer. The rotational population distribution of molecules desorbed was determined from  $1 + 1$  resonance enhanced multiphoton ionization (REMPI) spectra using a tunable ultraviolet laser and a microchannel plate ion detector.

A chromel–alumel thermocouple spot-welded to the back of the metal substrate was calibrated by sublimation of bulk krypton. We used 99.995% pure krypton from Cryogenic Rare Gas Laboratories or Liquid Carbonic. First, to check the pressure response of the mass spectrometer, we filled the chamber with Kr and compared the mass spectrometer current to an Ultek 8130 nude ion gauge. The chamber was then re-evacuated and the substrate cooled to about 25 K and dosed with Kr from the beam source. The surface was warmed to 35–40 K and the Kr flux and thermocouple voltage recorded at several points.

Over a wide pressure range, sublimation of the rare gases closely follows the Clausius–Clapeyron form  $\log(P) = A + B/T$ . For Kr, the coefficients are [9]:  $A = 7.73270$ , and  $B = -578.320$ . Inverting this equation gave us a temperature for each of our measured pressures, plotting this temperature against the thermocouple voltage we found a linear response:  $T$  (K) =  $85.77 V$  (mV) + 564, with  $\sigma = 0.6$  K.

Fig. 1a is a plot of Kr sublimation pressure versus thermocouple voltage, overlaid on the curve from the literature with its temperature axis scaled to match, and fig. 1b is the thermocouple calibration. Taking into account pressure measurement errors, thermocouple nonlinearity and extrapolation error, the surface temperature during NO sublimation was  $50 \pm 3$  K. Temperature stability, based on thermocouple precision and controller drift, was about 0.2 K.

In establishing the temperature, we equated the Kr signal in our mass spectrometer due to sublimation with the equilibrium vapor pressure. The reader may object that this begs the question, as it assumes quasi-equilibrium with cosine desorption and unit sticking. Furthermore, for the flux into the detector to equal that from an isotropic gas, the detector must view an area smaller than the desorbing region. The detector saw a 2.5 mm diameter circle, which was not entirely contained within the  $2 \times 4$  mm elliptical dosed spot. Nevertheless, this calibration scheme was sufficient, as the rare gas vapor pressure increases sharply with temperature, and a factor of two error in the pressure would change the calibration by only 1 K.

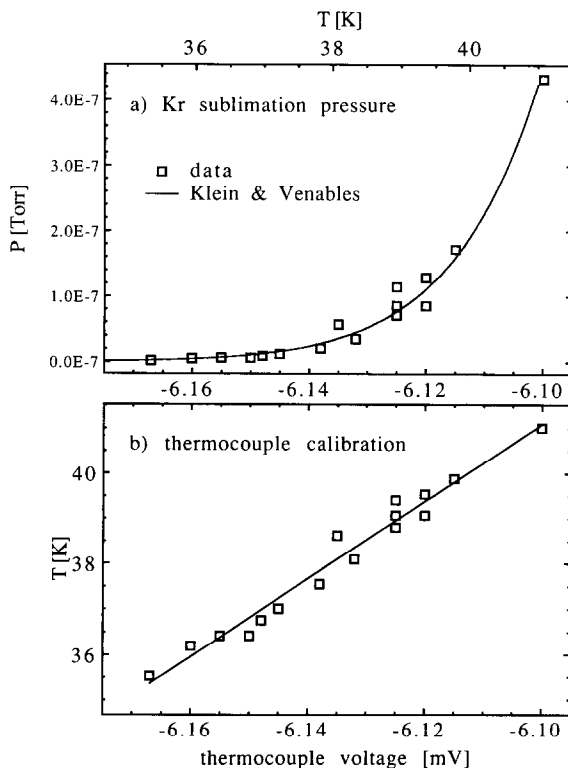


Fig. 1. The Chromel–Alumel thermocouple was calibrated from the sublimation pressure of bulk krypton. The solid line is a Clausius–Clapeyron form  $\log P = A + B/T$  with values from ref. [9]. Inverting this equation, we obtained a temperature at each pressure. The transformed data fits a linear voltage–temperature response.

To examine NO sublimation, we first cooled the substrate to about 25 K and dosed with a molecular beam of C.P. 99% grade NO from Matheson to condense a film of  $\sim 1000$  layers of NO solid. We then warmed the sample, and watched for NO sublimation with the mass spectrometer. The mass spectrometer used electron bombardment ionization followed by an Extranuclear quadrupole, and was doubly differentially ion pumped. It viewed the entire NO dosed region and could be rotated about an axis lying in the surface plane and passing through the dosed spot to obtain the angular distribution. At 50 K roughly one hundredth to one tenth of a layer desorbed each second. For these desorption rates the low density of molecules above the surface precludes collisions. At 50 K, obtaining a single REMPI spectrum took about 10 min, so only a fraction of the film was removed during the course of a spectrum measurement. The changing film thickness and the characteristics of the substrate were thus not expected to affect the desorption.

REMPI spectra of the  $\text{NO } A^2\Sigma^+ \leftarrow X^2\Pi\gamma(0-0)$  band required UV light near 225–227 nm, which was generated by a Quanta-Ray DCR-1  $\text{Nd}^{3+}$ -YAG laser pumping Florescein 548 in a PDL-1 dye laser, doubling the dye laser output in an angle tuned KDP crystal, and Raman shifting in a high pressure  $\text{H}_2$  cell. The second anti-Stokes order of the doubled light was selected by adjusting the angle of a quartz Pellin–Broca dispersing prism. A second Pellin–Broca prism with a mirror image orientation relative to the first insured that the angle of the selected beam did not vary with wavelength. A 61 cm focal length  $\text{CaF}_2$  entrance lens focused the laser through a Suprasil UHV window to the crystal 68–73 cm away producing a 0.5 mm diameter beam waist above the condensed NO. The laser beam was parallel to and  $\sim 5$  mm above the crystal surface and polarized  $45^\circ$  with respect to crystal normal.

Pulse energies were determined from the average power of the 10 Hz, 5 ns pulses measured with a Scientech 38-0101 power meter. Energy of  $300 \mu\text{J}$  or  $125 \text{ mJ}/\text{cm}^2$  of laser beam cross section resulted in a power density above the surface of  $25 \text{ MW}/\text{cm}^2$  with a factor of two uncertainty from the beam diameter. Measurements of ion signal versus laser power indicate that the power density was sufficient to saturate the  $\text{NO } A^2\Sigma^+ \leftarrow X^2\Pi$  bound to bound transition, but not to saturate the weaker  $\text{NO}^+ \leftarrow A^2\Sigma^+$  bound to free ionizing transition. We studied the single shot power dependence of the  ${}^2\Pi_{1/2} Q_1$ ,  $P_{21}$  bandhead and  $R_{21}$ ,  $J'' = 8.5$  transitions. Both fit a simple empirical saturation curve of the form  $S \propto I^2/(I - I_0)$ , and were well within the linear region for the laser power used, including fluctuations. Since the ion signal was linear in laser energy, signal and energy were averaged separately for 100–200 shots at each wavelength and normalized later. Full saturation simplifies analysis, but exacts a cost in resolution; spectra show a linewidth of about  $1.5 \text{ cm}^{-1}$  or  $0.075 \text{ \AA}$ .

Data acquisition was controlled by an LSI-11 compatible Charles River Data Systems minicomputer interfaced to the experiment via a Kinetic Systems CAMAC bus. We measured the ion signal, baseline and laser intensity for each shot. The ion pulse was detected and amplified with a modified Gallileo FTD 2001 microchannel plate mounted parallel to and 3.4 cm away from the surface, and digitized with a LeCroy 2249SG gated integrator A/D converter. 50 ns gates were generated by a KGE custom delay generator triggered by the laser Q-switch output. The laser energy for each shot was detected with an EG&G UV100BQ photodiode, then digitized. The dye laser wavelength was incremented by a stepping motor controller with a custom CAMAC interface. The typical wavelength increment was  $0.025 \text{ \AA}$  ( $0.4 \text{ cm}^{-1}$ ).

### 3. Results and analysis

The sticking coefficient for the molecular beam of NO, measured by the rise in total chamber pressure with and without the NO covered 50 K surface

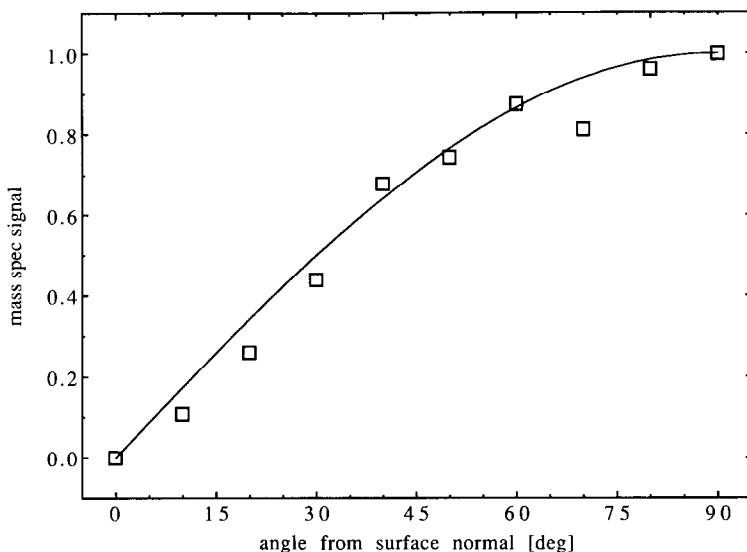


Fig. 2. The angular dependence of the NO sublimation flux is cosine with respect to the surface normal.

in the beam path, was  $> 0.9$ . Time of flight measurements revealed that a few percent of the beam was inelastically scattered, showing partial accommodation. When the surface was cooled to 35 K there remained only a small amount of elastic scattering, with a total sticking fraction over 0.99. These figures do not apply to an equilibrium 50 K gas – the molecular beam is supersonic with a stream velocity of  $7.6 \times 10^4$  cm/s and a velocity spread of  $1.1 \times 10^4$  cm/s, and the average translational energy in the beam corresponds to a temperature over 700 K. For equilibrium NO gas at 50 K, which we did not measure, we expect that sticking on bulk NO is very near unity.

At 50 K, on the order of  $10^{13}$ – $10^{14}$   $\text{cm}^{-2} \text{s}^{-1}$  NO molecules desorbed from the film. An Arrhenius plot of desorption rate versus temperature gave an activation energy of  $3.6 \pm 0.5$  kcal/mol. The angular flux distribution measured with the mass spectrometer was cosine with respect to surface normal, as shown in fig. 2.

The classic Hertz–Knudsen desorption rate

$$\frac{1}{A} \left( \frac{\partial N}{\partial t} \right)_T = sP_0 / \sqrt{2\pi mkT}, \quad (1)$$

is  $4.5 \times 10^{13}$   $\text{cm}^{-2} \text{s}^{-1}$  at 50 K, based on an equilibrium vapor pressure  $P_0 = 5 \times 10^{-8}$  Torr from thermodynamic data in the literature, ref. [10]:

$$-RT \ln P \text{ (atm)} = 3822 - 11.86T \log T + 0.034T^2 - 11.39T \text{ cal/mol.} \quad (2)$$

Desorption rates may be calculated from transition state theory (TST):

$$k_{\text{TST}} = \kappa \frac{kT}{h} \frac{q^\ddagger}{q_{\text{ads}}} e^{-\Delta E^\ddagger/kT}. \quad (3)$$

If the transition state is taken as the free gas phase molecule, any restriction on the motion of the adsorbate reduces its partition function and leads to a larger pre-exponential factor. This reasoning has been applied to desorption of NO from Pt(111) at low coverage, and suggests a hindered adsorbate [11].

We are unable to make similar arguments for NO sublimation. We know only the enthalpy of sublimation: from the literature [10]

$$\Delta H_{\text{sub}} = 3822 + 5.15T - 0.03T^2 \text{ cal/mol}, \quad (4)$$

which is 4.0 kcal/mol at 50 K; we measure  $3.6 \pm 0.5$  kcal/mol. A pseudo-first-order rate for sublimation using  $\Delta E^\ddagger = \Delta H_{\text{sub}}$  gives a pre-exponential factor of  $10^{16} \text{ s}^{-1}$ . But any application of transition state theory with this value will involve the partition functions for only the bulk solid and vapor. For ideal vapor, the TST rate is just the Hertz–Knudsen rate. To examine the surface partition function, we must have an appropriate desorption energy, which will not in general equal  $\Delta H_{\text{sub}}$ . When the surface free energy is significant, the actual desorption energy will be lower than  $\Delta H_{\text{sub}}$ , while for adsorption there may be an activation barrier. If the desorption energy is known, the transition state theory can give the surface partition function and an idea of the surface potentials from accurate measurements of the temperature dependent desorption rates.

There is of course one relevant quantity which may be determined by comparing experimental growth or evaporation rates to TST using bulk phase energetics – the sticking probability. The TST rate is a maximum; lower rates occur if there is recrossing of the transition surface. This is expressed in the transmission coefficient  $\kappa$ . A  $\kappa < 1$  may indicate dynamical constraints or a local potential minimum between the transition and product states. With an appropriate choice of transition state,  $\kappa$  may be identified with the sticking probability. By analogy, less than unit sticking may be due to dynamical restrictions, or to a real local minimum – a precursor state.

A correct treatment of evaporation as a zeroth-order process is presented in ref. [12]; for free evaporation we have:

$$\frac{dN}{dt} = -sA \frac{2\pi mkT\mu}{h^3} q_{\text{int}} e^{\mu/kT}, \quad (5)$$

where  $\mu$  is the chemical potential of the solid. This is essentially the Hertz–Knudsen rate with the statistical mechanical equilibrium vapor pressure  $P_0 = q_v/q_s$ . Using a Debye model

$$\mu = -\Delta H_{\text{sub}} + 3kT \ln(1 - e^{-\Theta/T}) - kT D(\Theta/T), \quad (6)$$

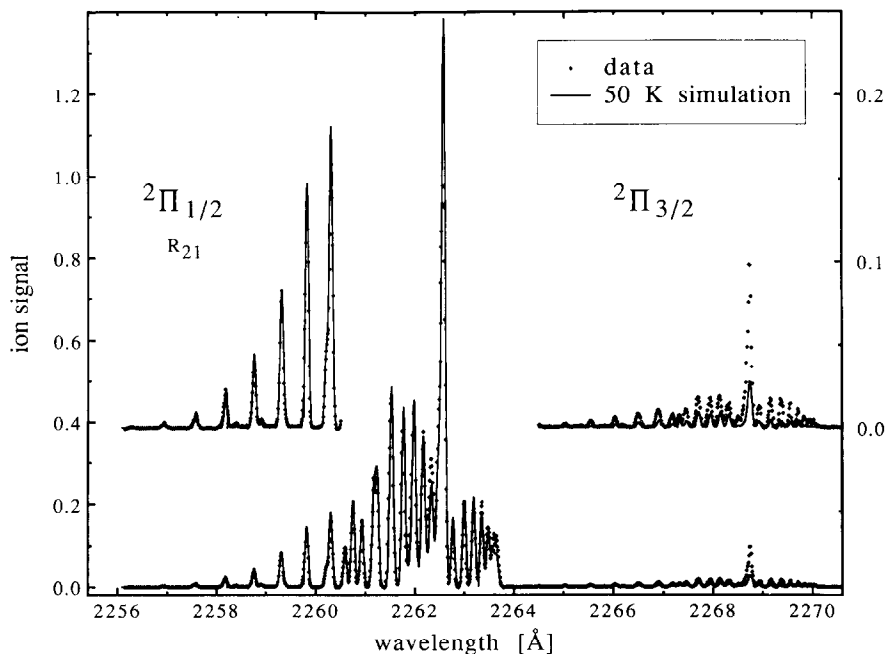


Fig. 3. Rotational spectrum of NO subliming at 50 K. The line is a simulation at 50 K. Note that the  ${}^2\Pi_{3/2}$  state is higher than the simulation. Deviation in the bandhead regions of both states may be due to use of a Gaussian lineshape in the simulation.

where  $\Theta$  is the Debye temperature, which can be derived from the heat capacity [10]:

$$C_p = 0.43 + 0.016T \text{ J/mol} \cdot \text{K}. \quad (7)$$

Assuming unit sticking, eq. (5) yields a desorption rate of  $5 \times 10^{13} \text{ cm}^{-2} \text{ s}^{-1}$ , consistent with our results. The use of  $\Delta H_{\text{sub}}$  here is appropriate, but again we have sacrificed any information about the nature of the surface dynamics. Kreuzer states [12]: “the condensation coefficient  $S_c$  contains all the information about the dynamics of the sticking process. It must either be taken from experiment or calculated in a statistical theory.”

Fig. 3 is the (1 + 1) REMPI spectrum of the NO  $A^2\Sigma^+ \leftarrow {}^2\Pi(0, 0)$  band. A simulated spectrum at 50 K is also shown. The simulation was for absorption, rather than REMPI, and weighted branches equally. It also used Gaussian lineshapes, which were not accurate in the bandhead regions where there was much overlap. The simulation is quite good in the tail of the  ${}^2\Pi_{1/2}$  state, where we also obtained the best rotational state information.

If we assumed a Boltzmann rotational distribution, single temperature fits of six spectra gave  $58 \pm 6 \text{ K}$ . Fitting the individual rotational state populations

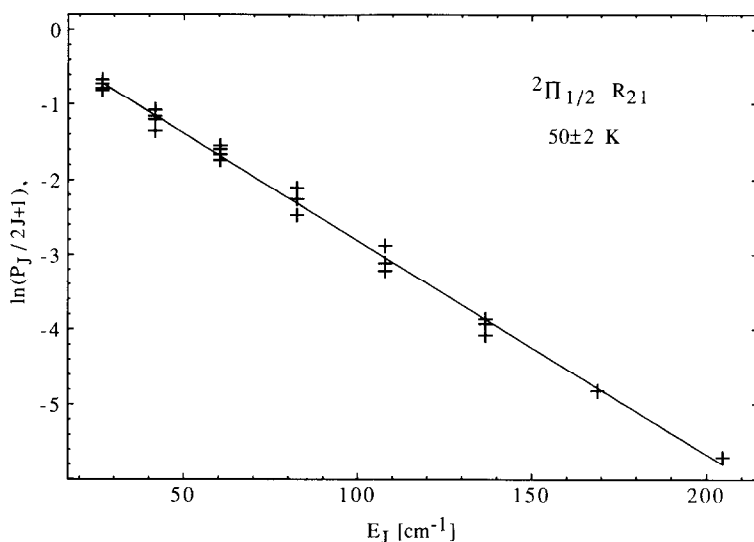


Fig. 4. Boltzman plot of the  $^2\Pi_{3/2} R_{21}$  branch rotational populations. The fit is  $50 \pm 2 \text{ K}$  ( $2\sigma$ ).

for all branches of the  $^2\Pi_{3/2}$  state for several spectra gave a temperature of  $54 \pm 2 \text{ K}$ . Both these treatments may introduce errors by neglecting intermediate state alignment for the different branches [13].

To simplify population analysis we looked at isolated lines from a single branch,  $R_{21}$ , so we could neglect overlap and intermediate state alignment, and still obtain a reliable value for the rotational populations. The effect of noise was reduced by taking the areas of Gaussian fits to each line. The Boltzmann plot of  $\ln[P_J / (2J + 1)]$  versus  $E_J$  gives a temperature of  $50 \pm 2 \text{ K}$ , fig. 4.

State specific scattering and desorption can be very sensitive to the details of the system. NO scattered from NO covered Pt(111) at 290 K is translationally accommodated [14], and NO thermally desorbed from Pt(111) is rotationally accommodated [15], though the rotations are aligned relative to the surface [16]. On the other hand, rotational scattering of NO from Ag(111) is not Boltzmann and shows rainbows at high  $J$  [6], and rotational populations of NO desorbing from monolayer coverage on Ru(100) deviate from the surface temperature above 500 K [5].

In response to the experiments showing non-Boltzmann rotational distributions, models of rotational energy changes during desorption have been proposed [17,18]. We examined the predictions of a few models at low temperatures. Gadzuk et al. propose a hindered to free rotor transition, in which zero point energy gives rise to rotational excitation. This leads to rotational populations independent of the surface temperature at low  $J$ , contrary to our results.

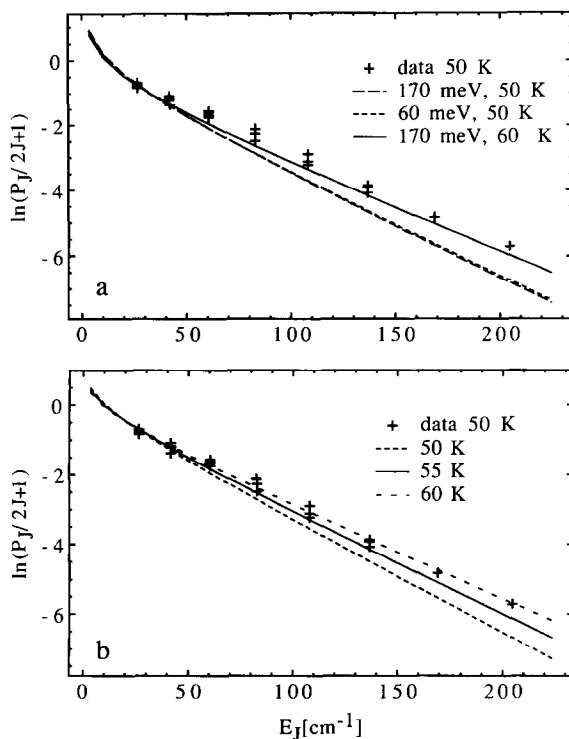


Fig. 5. Boltzmann plots of final rotational distribution for two simple models of rotationally induced desorption. (a) Model from ref. [17]. The first two curves are for a 50 K surface with binding energies corresponding to  $\Delta H_{\text{sub}}$  (170 meV), and the NO dimer energy minus  $kT$  (60 meV). The third curve is for a surface at 60 K. (b) “P” transition model,  $\Delta J = -1$ . The curves are for surface temperatures of 50, 55 and 60 K.

Bowman and Gossage’s model begins with a free rotor whose rotational energy is used for desorption. They obtain a simple result for the final rotational populations:

$$P_{J'} = \left[ (2J' + 1)^2 + 4\Delta(T)/B \right]^{1/2} \exp(-\Delta(T)/RT) \times \exp[-BJ'(J' + 1)/RT] / Q_r(T), \quad (8)$$

where  $B$  is the rotational constant and  $\Delta(T) = D - (E_v)$  is an effective binding energy based on the well depth and average vibrational energy for a Morse potential. Results for a few binding energies and initial temperatures are shown in fig. 5a. If the binding energy is taken as  $\Delta H_{\text{sub}}$ , or even a third of this value, which is roughly the  $(\text{NO})_2$  dimer dissociation energy, there is no agreement. If the actual surface temperature were 60 K, the curve can be made to fit the data, but this is outside our temperature error limits. Even so, the

plot is still clearly non-Boltzmann, in contrast to the data, which is fit well by a line.

This model was only intended to apply where a large fraction of molecules have enough energy to desorb. Where  $kT$  is much lower than the well depth, only molecules in the tail of the thermal distribution can desorb, for NO at 50 K this is only one in  $10^{18}$  molecules. For the relevant states near the top of the well, the energy required to escape will approach the rotational spacing, and the transition must be quantized. Suppose desorbing molecules are again free rotors at  $T_s$ , near the top of the adsorbate surface well, so that a single rotational transition allows escape, and the transition probability is independent of initial  $J$ . For these “ $P$ ” transitions,  $\Delta J = -1$ , the final distribution is:

$$P_{J'} = (2J' + 3) \exp[-B(J' + 2)/RT] / Q_r(T). \quad (9)$$

This distribution is shown in fig. 5b for several surface temperatures. It might fit the data if the surface were 5 K hotter than we measured, which is within possible error. It is again non-Boltzmann, but the deviation is most pronounced at low  $J$  ( $J = 0$  is missing), which we cannot measure well, as they are near the bandheads. A more quantal system,  $H_2$  sublimation at low enough temperatures, might show evidence for rotationally mediated desorption.

In fig. 3, the observed  ${}^2\Pi_{3/2}$  intensity is greater than expected from the simulation. The electronic temperature of the desorbed NO may have been higher than the surface temperature the  ${}^2\Pi_{1/2}$  and  ${}^2\Pi_{3/2}$  spin-orbit states, separated by  $123 \text{ cm}^{-1}$ , had a population ratio corresponding to  $70 \pm 12 \text{ K}$ . We were unable to find instrumental non-linearities or errors in data analysis which might account for this result, and are unaware of any possible spectroscopic origin.

There may be subtle intramolecular effects influencing the spin-orbit distribution. When NO dimer is photodissociated by infrared vibrational excitation of the  $\nu_1$  or  $\nu_4$  NO stretching modes around  $1800 \text{ cm}^{-1}$ , the product  ${}^2\Pi_{1/2}$  to  ${}^2\Pi_{3/2}$  ratio depends on the mode excited [19]. We have no model for desorption at lower energies which would favor the  ${}^2\Pi_{3/2}$  state.

The polarization or alignment of rotations relative to the surface was not determined [16].

#### 4. Discussion

Many of the experimental techniques of surface science are being pushed beyond simple surfaces to disordered, amorphous and liquid materials, and to interfaces undergoing phase transitions or otherwise out of equilibrium. Interpretation of such experiments may be difficult, as current theories of surface dynamics, scattering and adsorption-desorption work best for single crystal surfaces with low adsorbate coverages [20]. Hence the important applied

technologies of evaporation, condensation and crystal growth have usually neglected the microscopic dynamics of the surface. There has been a tendency to “reduce the role of the interface to a parameter in the transport boundary conditions” [21]. For processes far from equilibrium, such as molecular beam epitaxy (MBE), or chemical vapor deposition (CVD), the detailed interfacial dynamics may be crucial. For instance, dynamical roughening of the surface, which certainly changes sticking probabilities, is seen in solid-on-solid models of crystal growth [22]. While it is possible that the condensation coefficient for all clean liquid surfaces is unity [23], accommodation may still fail for hyperthermal molecules, as we observed in scattering a supersonic molecular beam of NO from amorphous solid NO. For non-equilibrium interfaces, if accommodation depends on the detailed molecular state distribution, or the net sticking probability changes during growth or evaporation, the microscopic dynamics must be considered explicitly.

The principle of detailed balance, which has been very useful in interpreting surface experiments [24,25], is relevant so long as the surface maintains local equilibrium, which may not always be the case. It is not clear in general how changes in ambient vapor pressure may affect surface structure and dynamics. For instance, the surface tension of a liquid metal may depend on the overlying vapor pressure [26]. As differential pumping methods enable studies of surfaces at higher vapor pressures, deviations from equilibrium should be considered. The surface may not retain its equilibrium morphology and thermal and density gradients may arise both at the surface and in the adjacent vapor. Strictly, detailed balance for transition probabilities always holds, but the observed rates depend on the populations, which will then be perturbed, and extrapolation to equilibrium conditions may not be valid. The microscopic relaxation at the surface is very rapid however, and with the exception of fast laser excitation [8] or slow surface phase transitions [27], local equilibrium should hold [28,29], and the methods of non-equilibrium thermodynamics will apply.

We have applied UHV surface methods and gas phase laser spectroscopy to a condensed material undergoing a phase transition, looking at desorbed molecules as a probe of surface dynamics. In this experiment, NO monomer sublimed into vacuum from bulk condensed NO at 50 K, exhibiting a cosine angular flux and Boltzmann rotational distribution at the surface temperature. In a study of the evaporation of Na<sub>2</sub> dimers from liquid Na, Miksch and Weber observed vibrational and rotational temperatures matching the bulk temperature [30]. Such results are not unexpected, but as Comsa and David [24] have clearly explained, even at equilibrium, desorption distributions need not be Boltzmann and cosine, provided scattering is such that the net distribution leaving the surface match that of the equilibrium vapor. Since the equilibrium vapor pressure of NO is  $5 \times 10^{-8}$  Torr at 50 K, fluxes are probably too low to significantly perturb the surface and we can use detailed

balance to relate our desorption distributions to sticking coefficients at equilibrium. We thus interpret our results as indicating that sticking probabilities for NO on NO solid do not depend on incident angle or rotational state, at least for those states populated at 50 K. We cannot rule out the possibility of a spin-orbit state dependent effect and did not measure rotational polarization or orientation.

From non-thermal distributions, accommodation and desorption dynamics might be deduced. In contrast, we observe simple Boltzmann and cosine distributions. Rigorously we can conclude only that, for the states observed, the sticking probability is independent of angle or rotational level. An equilibrium distribution such as we have obtained contains a minimum of information, allowing us to rule out desorption models which are clearly non-Boltzmann, but little else. A suddenly unhindered rotor does not seem to work, and we might propose that the surface molecules are free rotors prior to desorption. But neither do we see evidence of a rotation to translation desorption mechanism. A small population of thermally excited molecules at the surface may be weakly bound, freely rotating and mobile. In desorption of low coverage adsorbates from crystal surfaces it has been suggested that the *absence* of the dynamical effects in desorption indicates a gas-like transition state or precursor [31]. For bulk condensed materials, desorptions might occur from a "self adsorbed" surface phase, 2D gas if desorption is continuous, or gas-solid coexistence as desorption occurs layer by layer. Or the surface of a subliming solid or evaporating liquid might be rough or heterogeneous on a molecular scale. Then one of Maxwell's original concepts may apply, that of a very rough surface causing multiple scattering and equilibration during adsorption or desorption [4]. While these pictures are plausible in light of equilibrium surface melting and molecular dynamics simulations [32], we cannot draw such conclusions from this experiment alone.

These ideas could be tested by more direct measurements of the structure, energetics and dynamics of the surfaces of liquids and amorphous or glassy solids. Ellipsometry, reflection high energy electron diffraction, helium reflectivity [33] and glancing incidence X-ray methods may indicate roughening or the existence of surface phases. Knowledge of the surface free energy is basic to any thermodynamic or statistical calculation such as transition state theory. Where the surface tension cannot be measured by conventional methods the surface partition function can be determined by comparison of bulk and surface phonon spectra. Quasi-elastic helium or neutron scattering could measure surface diffusion rates and mobilities, but very good energy resolution is required. Surface sensitive X-ray and optical techniques can still be used where increasing vapor pressures prohibit scattering techniques, but as collisions become significant, we can no longer examine the unperturbed dynamics of desorbing molecules.

As our experimental skill and theoretical insight increase, the molecular

nature of evaporation and condensation, which Maxwell and Hertz wondered about a century ago, continues to present challenges.

## Acknowledgements

This work was supported in part by the Office of Naval Research, and the the National Science Foundation–Materials Research Laboratory Program at the University of Chicago (NSF-DMR-8519460). S.J.S. also acknowledges research support from the Louis Block Fund at the University of Chicago, and D.F.P. thanks the Xerox Corp. for partial fellowship support.

## References

- [1] H. Hertz, *Ann. Phys.* 17 (1882) 177.
- [2] R. Marcelin, *Compt. Rend. (Paris)* 158 (1914) 1419.
- [3] M. Knudsen, *Ann. Phys.* 47 (1915) 697.
- [4] J.C. Maxwell, *Phil. Trans.* 170 (1879) 231.
- [5] D.S. King and R.R. Cavanaugh, *J. Chem. Phys.* 76 (1982) 5634.
- [6] A.W. Kleyn, A.C. Luntz and D.J. Auerbach, *Phys. Rev. Letters* 47 (1981) 1169.
- [7] C.-F. Yu, K.B. Whaley, C.S. Hogg and S.J. Sibener, *J. Chem. Phys.* 83 (1985) 4217.
- [8] W.C. Natzle, D. Padowitz and S.J. Sibener, *J. Chem. Phys.* 88 (1988) 7975.
- [9] M.L. Klein and J.A. Venables, *Rare Gas Solids*, Vol. 2 (Academic Press, New York, 1976) pp. 687–689.
- [10] US Bureau of Mines Bulletin 601 US Department of Commerce (1962).
- [11] C.W. Muhlhause, L.R. Williams and J.C. Tully, *J. Chem. Phys.* 83 (1985) 2594.
- [12] H.J. Kreuzer, R.G. Chapman and N.H. March, *Phys. Rev. A* 37 (1988) 582.
- [13] D.C. Jacobs, R.J. Madix and R.N. Zare, *J. Chem. Phys.* 85 (1986) 5469.
- [14] F. Frenkel, J. Hager, W. Kreiger, H. Walther, C.T. Campbell, G. Ertl, H. Kuipers and J. Segner, *Phys. Rev. Letters* 46 (1981) 152.
- [15] D.A. Mantell, R.R. Cavanaugh and D.S. King, *J. Chem. Phys.* 82 (1985) 1046.
- [16] D.C. Jacobs, K.W. Kolasinski, R.J. Madix and R.N. Zare, *J. Chem. Phys.* 87 (1987) 5038.
- [17] J.M. Bowman and J.L. Gossage, *Chem. Phys. Letters* 96 (1983) 481.
- [18] J.W. Gadzuk, U. Landman, E.J. Kuster, C.L. Cleveland and R.N. Barnett, *Phys. Rev. Letters* 49 (1982) 426.
- [19] M.P. Casassa, J.C. Stephenson and D.S. King, *J. Chem. Phys.* 89 (1988) 1966.
- [20] H.J. Kreuzer and Z.W. Gortel, *Physisorption Kinetics* (Springer, Berlin, 1986).
- [21] B. Mutaftschiev, Ed., *Interfacial Aspects of Phase Transitions* (Reidel, Dordrecht, 1982).
- [22] G.H. Gilmer and K.A. Jackson, in: *Current Topics in Materials Science*, Vol. 2, Eds. E. Kaldis and H.J. Scheels (North-Holland, Amsterdam, 1977).
- [23] H.K. Cammenga, in: *Current Topics in Materials Science*, Vol. 5, Ed. E. Kaldis (North-Holland, Amsterdam, 1980).
- [24] G. Comsa and R. David, *Surface Sci. Rept.* 5 (1985) 145.
- [25] M.J. Cardillo, M. Balooch and R.E. Stickney, *Surface Sci.* 50 (1975) 263.
- [26] D.W.G. White, *Trans. Met. Soc. AIME* 796 (1966) 236.
- [27] S.H. Payne and H.J. Kreuzer, *Surface Sci.* 205 (1988) 153.
- [28] I. Kuščer, *Surface Sci.* 25 (1971) 225.
- [29] E.P. Wenaas, *J. Chem. Phys.* 54 (1971) 376.

- [30] G. Miksch and H.G. Weber, *Chem. Phys. Letters* 87 (1982) 544.
- [31] D. Menzel, Z.W. Gortel and H.J. Kreuzer, in: *Kinetics of Interface Reactions*, Eds. M. Grunze and H.J. Kreuzer (Springer, Berlin, 1987).
- [32] J.F. van der Veen and M.A. Van Hove, Eds., *The Structure of Surfaces II*, Vol. 11 of Springer Series in Surface Sciences (Springer, Berlin, 1988).
- [33] B. Poelsema, L.K. Verheij and G. Comsa, *Phys. Rev. Letters* 51 (1983) 2410.